MOLECULAR AND CELLULAR BIOLOGY, Aug. 2004, p. 6635–6644 Vol. 24, No. 15
0270-7306/04/$08.00+0 DOI: 10.1128/MCB.24.15.6635–6644.2004

Gene Targeting Reveals a Widespread Role for the High-Mobility-Group Transcription Factor Sox11 in Tissue Remodeling

Elisabeth Sock,[1] Stefanie D. Rettig,[1] Janna Enderich,[1] Michael R. Bösl,[2] Ernst R. Tamm,[3] and Michael Wegner[1]*

Institut für Biochemie[1] and Institut für Anatomie,[3] Universität Erlangen-Nürnberg, Erlangen, and Max-Planck-Institut für Neurobiologie, Martinsried,[2] Germany

Received 10 March 2004/Returned for modification 24 April 2004/Accepted 11 May 2004

The high-mobility-group domain-containing transcription factor Sox11 is expressed transiently during embryonic development in many tissues that undergo inductive remodeling. Here we have analyzed the function of Sox11 by gene deletion in the mouse. *Sox11*-deficient mice died at birth from congenital cyanosis, likely resulting from heart defects. These included ventricular septation defects and outflow tract malformations that ranged from arterial common trunk to a condition known as double outlet right ventricle. Many other organs that normally express Sox11 also exhibited severe developmental defects. We observed various craniofacial and skeletal malformations, asplenia, and hypoplasia of the lung, stomach, and pancreas. Eyelids and the abdominal wall did not close properly in some *Sox11*-deficient mice. This phenotype suggests a prime function for Sox11 in tissue remodeling and identifies *SOX11* as a potentially mutated gene in corresponding human malformation syndromes.

Transcription factors of the Sox protein family are characterized by the possession of a subtype of high-mobility-group domain which allows sequence-specific binding to the minor groove of DNA (31). This domain was first identified in Sry, the prototypic family member involved in male sex determination. Over the last few years, many Sox proteins have been shown to be involved as regulators in diverse developmental processes ranging from epiblast formation to the terminal differentiation of certain cell types (3, 31).

The 20 Sox proteins which have been identified in mammals can be further subdivided into eight groups (groups A to H) according to their degrees of similarity both within and outside the high-mobility-group domain. Mammalian group C, for instance, consists of the three highly related proteins Sox4, Sox11, and Sox22. Sox4 has been studied extensively in vivo and has been shown to be essential for pro-B-cell expansion and for the formation of semilunar valves and of the outflow tract from the endocardial ridges of the heart (25). Further nonessential roles for Sox4 have been defined in thymocyte differentiation (24).

Much less is known about the biological role of Sox11 and Sox22. Species in which Sox11 has been identified include humans, mice, rats, chickens, *Xenopus laevis*, and zebra fish (11, 14, 15, 17, 21, 22, 30). Sox11 functions as a strong transcriptional activator in tissue culture systems and possesses a transactivation domain at its extreme carboxy terminus with a high level of homology to the corresponding region of Sox4 (17).

The expression of Sox11 has also been studied in several species. In zebra fish, in which two Sox11 orthologs exist because of the recent whole-genome duplication in teleosts, Sox11 transcripts are maternally inherited (22). In all species analyzed, Sox11 is present during gastrulation and early postgastrulation development throughout the embryo, with the notable exception of the heart (14, 17, 22). Later during development, Sox11 is prominently expressed in the developing nervous system in both glial and neuronal lineages and at many sites throughout the embryo where epithelial-mesenchymal interactions occur (14, 17, 30). At sites of such epithelial-mesenchymal interactions, Sox11 can be found in the mesenchymal or epithelial compartment, and it has been postulated to be involved in inductive remodeling (14). Its expression quite often exhibits a dynamic pattern with regards to both expression sites and expression levels. In several tissues, Sox11 exhibits an expression profile that is very similar to that of the highly related Sox4 protein (7, 17), whereas in other tissues, the occurrence of both proteins is complementary (18). Sox11 expression in most tissues is transient. As a consequence, there is little Sox11 expression in the adult, in contrast to its widespread occurrence during embryogenesis. Here we have started to study the role of Sox11 during mouse development by generating a Sox11-deficient mouse model. This model yields important insights into the biological role of Sox11.

MATERIALS AND METHODS

Construction of targeting vector. The genomic sequence for the *Sox11* locus of 129/Sv mice was obtained by screening a lambda phage library. A 2.3-kb fragment immediately upstream of the translation start was used as a 5′ homology region. The start codon of the β-galactosidase marker (LacZ) with a nuclear localization signal was placed exactly over the start codon of *Sox11*. A 5-kb fragment starting 400 bp downstream of the open reading frame was used as a 3′ homology region. The combination of the 5′ homology region and LacZ and the 3′ homology region were inserted into pTVO on either side of the neomycin resistance cassette (Fig. 1A). The targeting vector thus replaced the complete open reading frame of *Sox11* with a β-galactosidase marker gene. The construct was linearized with NotI before electroporation.

* Corresponding author. Mailing address: Institut für Biochemie, Fahrstrasse 17, D-91054 Erlangen, Germany. Phone: 49 9131 85 24620. Fax: 49 9131 85 22484. E-mail: m.wegner@biochem.uni-erlangen.de.

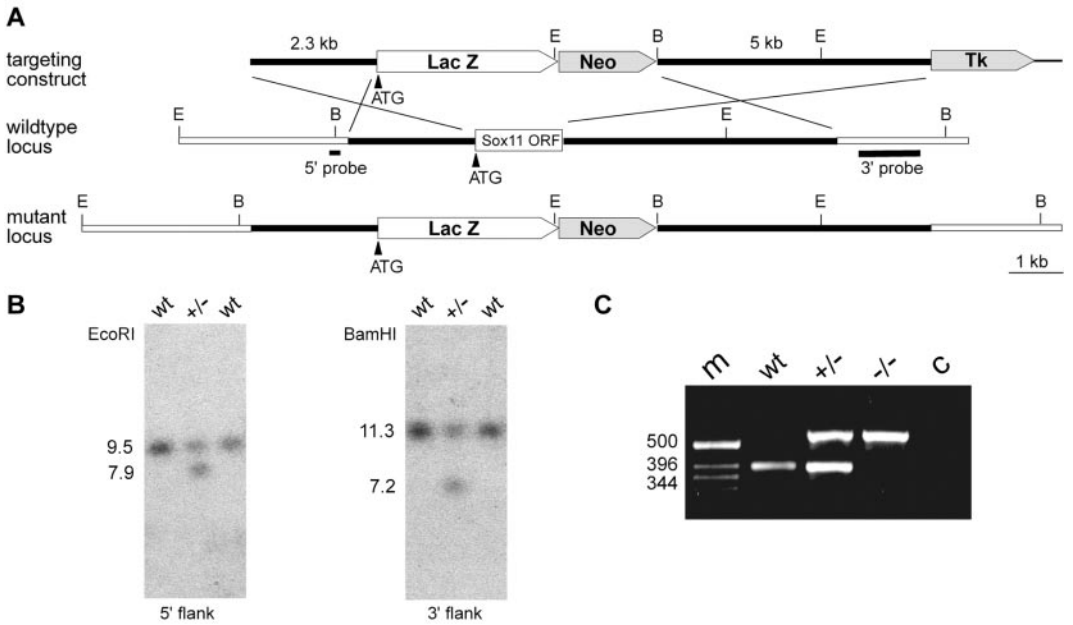

FIG. 1. Targeted disruption of *Sox11* in mice. (A) Schematic representation of the targeting construct (top), the *Sox11* wild-type locus (middle), and the mutant locus (bottom). The *Sox11* open reading frame is shown as a box, with flanking regions shown as bars. Regions of homology between the wild-type locus and the targeting vector are depicted as black bars, and surrounding genomic regions that are not contained in the targeting construct are depicted as white bars. Plasmid backbone sequences of the targeting construct are indicated by thick lines. Restriction sites for BamHI (B) and EcoRI (E) are shown, as are the locations of the 5′ and 3′ probes and the start codon of the *Sox11* gene (ATG). LacZ, gene for β-galactosidase; Neo, neomycin resistance selection cassette; Tk, herpes simplex virus thymidine kinase gene cassette. (B) Southern blot analysis of DNAs from wild-type (wt) and heterozygous (+/−) ES cells digested with EcoRI for use with the 5′ probe or with BamHI for use with the 3′ probe. The sizes of bands corresponding to the wild-type and targeted alleles are indicated. (C) PCR-based genotyping of wild-type (wt), heterozygous (+/−), and *Sox11*-deficient (−/−) embryos at 18.5 dpc. The sizes of DNA fragments (in base pairs) in the DNA size marker (m) are indicated to the left of the agarose gel. c, control without added genomic DNA.

Gene targeting and generation of mouse mutants. The linearized construct was electroporated into R1 embryonic stem (ES) cells (129 X1 × 129 S1), which were then selected with G418 (200 μg per ml) and ganciclovir (2 μM). Selected ES cell clones were screened by Southern blotting with a 0.2-kb 5′ probe which recognized a 9.5-kb fragment of the wild-type allele and a 7.9-kb fragment of the targeted allele in genomic DNA digested with EcoRI (Fig. 1A and B). Appropriate integration of the 3′ end of the targeting construct was verified by using a 1.0-kb 3′ probe on ES cell DNA digested with BamHI. This probe hybridized to a 7.2-kb fragment in the targeted allele, as opposed to an 11.3-kb fragment in the wild-type allele (Fig. 1A and B). Three targeted ES cell lines were injected into blastocysts to generate chimeras. Chimeric males from all three independent clones transmitted the targeted allele to their offspring. No differences were detected among mice derived from the different ES cell lines. Homozygous mutant mice were generated by intercrosses of heterozygous animals. Genotyping was routinely performed by PCR analysis (Fig. 1C), using a common upper primer located 21 to 40 bp upstream of the start codon (5′-GCC CGC GCA GGA GAC CGA GC-3′) and two lower primers located 329 to 350 bp (5′-CTT GTA GTC GGG GTA GTC AGC C-3′) and 494 to 513 bp (5′-TAA AAA TGC GCT CAG GTC AA-3′) downstream of the start codon in *Sox11* and *lacZ*, respectively. DNAs were obtained from tail tips, or in the case of embryos, from yolk sacs. PCRs were performed in 20-μl reaction mixtures containing standard buffer, 5% dimethyl sulfoxide, and a 0.25 μM concentration of each primer. The cycling conditions consisted of an initial 1-min denaturing step at 94°C, followed by 35 cycles of 30 s at 94°C, 30 s at 58°C, and 30 s at 72°C. A 390-bp fragment was indicative of the wild-type allele, and a 553-bp fragment was indicative of the targeted allele. All analyses described in this paper were performed on littermates of the F_2-F_4 generation.

X-Gal and histological staining procedures and scanning electron microscopy. Embryos were isolated at 9.5 to 18.5 days postconception (dpc) from staged pregnancies. After fixation in 1% paraformaldehyde, the β-galactosidase activity was detected in whole-mount embryos and cryotome sections (10 to 25 μm) by incubation for several hours at 37°C in 1% X-Gal (5-bromo-4-chloro-3-indolyl-β-D-galactopyranoside) until blue precipitates were detectable (28). For hematoxylin-eosin staining, embryos were incubated overnight in 4% paraformaldehyde, dehydrated, embedded in paraffin, sectioned on a microtome to a 3-μm thickness, dewaxed, rehydrated, and consecutively stained in Mayer's hematoxylin and eosin.

For the staining of cartilage and bones, skeletons were incubated at room temperature for 4 h in a solution containing alcian blue, 20% acetic acid, and 80% ethanol, fixed in ethanol, and consecutively stained for 4 h in alizarin red S–1% KOH. After being cleared in 2% KOH, the skeletons were stored in 80% glycerol (27).

For scanning electron microscopy, embryonic hearts (18.5 dpc) were fixed overnight in a cacodylate-buffered fixative containing 4% paraformaldehyde, 4% glutaraldehyde, and 0.05% picric acid (pH 7.3). After postfixation in cacodylate-buffered 1% osmium tetroxide for 3 h and dehydration in ascending ethanol and acetone series, the specimens were critical point dried, sputter coated with gold-palladium, and investigated with a Stereoscan 90 scanning electron microscope (Cambridge, United Kingdom).

RESULTS

Targeted removal of Sox11 gene. The mouse *Sox11* gene is localized as an intronless gene on chromosome 12. For gene deletion, we replaced the complete open reading frame of *Sox11* with a β-galactosidase marker gene (Fig. 1A, LacZ) as described in Materials and Methods. As expected from the complete deletion of all *Sox11* coding sequences, we failed to detect gene-specific transcripts by reverse transcription-PCR in Sox11-deficient embryos when primers for regions within the open reading frame were chosen (data not shown).

An analysis of β-galactosidase expression in $Sox11^{+/-}$ mice by X-Gal staining revealed that β-galactosidase reproduced the spatial expression pattern of *Sox11* during development.

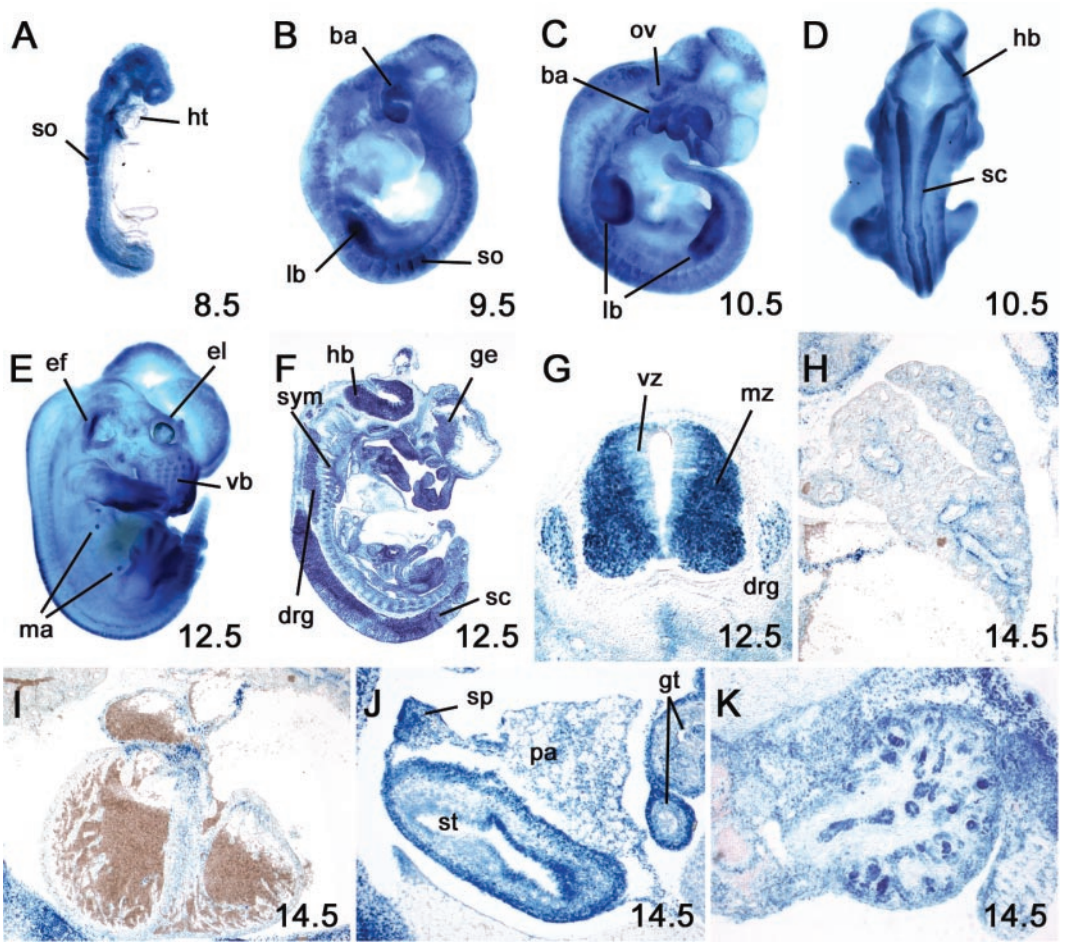

FIG. 2. Developmental expression of β-galactosidase marker gene integrated into *Sox11* gene locus. β-Galactosidase activity was detected colorimetrically with the X-Gal substrate in whole-mount (A to E) and cryotome-sectioned (F to K) heterozygous embryos at 8.5 dpc (A), 9.5 dpc (B), 10.5 dpc (C and D), 12.5 dpc (E to G), and 14.5 dpc (H to K). No X-Gal staining was detected in wild-type littermates under identical conditions. Abbreviations: ba, branchial arches; drg, dorsal root ganglia; ef, earflap; el, eye lid; ge, ganglionic eminence; gt, gut; hb, hindbrain; ht, heart; lb, limb bud; ma, mammary anlage; mz, mantle zone of the spinal cord; ov, otic vesicle; pa, pancreas; sc, spinal cord; so, somite; sp, spleen; st, stomach; sym, sympathetic chain ganglia; vb, vibrissae; vz, ventricular zone of the spinal cord.

This included early ubiquitous expression throughout the embryo, with the exception of the heart (Fig. 2A); upregulation in somites (Fig. 2A and B), branchial arches (Fig. 2B and C), the central nervous system (Fig. 2D, F, and G), the peripheral nervous system (Fig. 2F and G), and the limb buds (Fig. 2B and C); and expression during later phases of embryonic development in many organs and tissues, including vibrissae, mammary buds (Fig. 2E), lungs (Fig. 2H), the stomach, the pancreas, the spleen (Fig. 2J), and kidneys (Fig. 2K). At later times of development, β-galactosidase was also found in the heart, with the highest levels being present in the outflow tract region (Fig. 2I). β-Galactosidase expression was less useful for studying the temporal profile of *Sox11* expression, as it persisted after *Sox11* had already been downregulated in the respective tissues.

Congenital cyanosis of *Sox11*-deficient mice. Heterozygous mice were readily obtained. They were viable, fertile, and could be intercrossed to generate Sox11-deficient mice. When genotyping was performed prenatally on litters obtained from staged pregnancies during either mid or late embryogenesis (Fig. 1C), *Sox11*-deficient embryos were obtained at expected Mendelian frequencies (Fig. 3A). However, *Sox11*-deficient mice were not found when litters from such intercrosses were genotyped at the time of weaning (Fig. 3B), suggesting that *Sox11* deficiency is lethal during the first postnatal weeks.

A closer inspection revealed that *Sox11*-deficient mice were born alive. However, death occurred immediately after birth. *Sox11*-deficient newborns exhibited, on average, a significant 23% reduction in birth weight relative to their wild-type and heterozygous littermates (Fig. 3C). Despite the fact that *Sox11*-deficient newborns responded to tactile stimuli, their breathing remained sporadic and irregular so that they rapidly became cyanotic (Fig. 3D) and succumbed to death. Furthermore, 97% of all *Sox11*-deficient mice exhibited an eyelid closure defect of variable severity around the time of birth (Fig. 3E to G) that could be used for rapid identification.

Congenital cyanosis often results from pulmonary insufficiency or a cardiovascular malfunction. An inspection of *Sox11*-deficient embryos and newborns revealed a significant hypoplasia of the lung which never filled the pleural cavity (Fig. 4A and B). Hypoplasia affected all lobes of the lung. The right

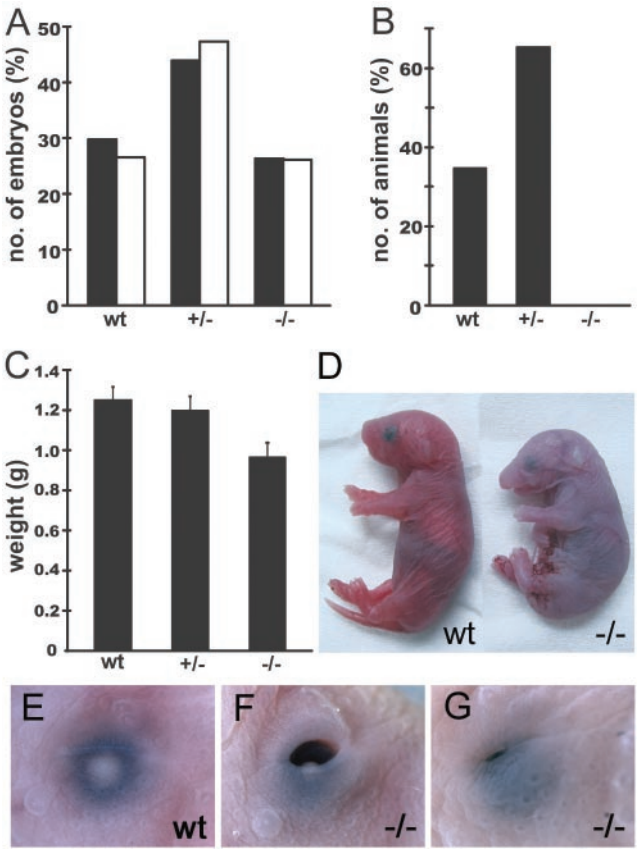

FIG. 3. Distribution of genotypes and birth weights in *Sox11*-deficient embryos and control littermates. (A) Embryos isolated between 8.5 and 15.5 dpc (filled bars [$n = 262$]) and between 16.5 and 18.5 dpc (open bars [$n = 222$]) were grouped according to genotype as wild-type (wt), heterozygous (+/−), or *Sox11*-deficient (−/−). The relative contribution of each genotype is indicated. (B) Relative genotype distribution of 3-week-old mice ($n = 98$). (C) Body weights were determined (in grams) for embryos at 18.5 dpc after delivery by caesarean section (17 wild-type embryos, 31 heterozygous embryos, and 25 *Sox11*-deficient embryos). The mean body weight (± standard error of the mean [SEM]) is presented for each genotype. (D) Gross morphology of embryos at 18.5 dpc after delivery by caesarean section. Note the smaller size, facial malformations, and cyanotic appearance of the *Sox11*-deficient embryo. (E to G) Eyelid closure defects in *Sox11*-deficient mice (F and G) compared to a control littermate (E) at 18.5 dpc.

accessory lobe, for instance, was strongly diminished in size and additionally exhibited several fissures instead of the usually even contours. A histological examination of late prenatal lungs additionally revealed significantly decreased diameters for most conducting airways (Fig. 4C and D). On average, the number of cell layers which separated immediately adjacent airways was increased in *Sox11*-deficient mice (Fig. 4E and F). The development of alveolar cell types appeared normal by histology and marker gene expression (data not shown). The observed defects in lung morphology might contribute to the immediate postnatal death.

Congenital heart defects. We next turned our attention to the heart. Sections through the hearts of *Sox11*-deficient mice revealed a ventricular septation defect. Differences in severity notwithstanding, this septation defect was fully penetrant. While at 12.5 dpc, the septum still grew from the posterior to the anterior pole of the heart to separate the left ventricle from the right ventricle (Fig. 5A and B), septation was essentially complete at 13.5 dpc in wild-type embryos (Fig. 5C). In their *Sox11*-deficient littermates, however, the ventricular septum had not closed at 13.5 dpc (Fig. 5D). All *Sox11*-deficient embryos analyzed at 14.5 or 18.5 dpc still exhibited this ventricular septation defect, which argues against a mere developmental delay (Fig. 5E to H).

In addition to the ventricular septation defect, there were malformations of the cardiac arterial outflow tract in all *Sox11*-deficient embryos analyzed. Light and scanning electron microscopy of the hearts of wild-type mice at 18.5 dpc showed that the pulmonary trunk and aorta were clearly separated and originated from their typical positions (Fig. 6A and C). In contrast, a single arterial trunk was frequently observed in *Sox11*-deficient embryos which originated from the right ventricle and was continuous with the descending aorta, which was situated on the left side (Fig. 6B and D).

For a closer examination of the defects at the arterial pole, the hearts of a total of six *Sox11*-deficient 18.5-dpc embryos were studied histologically in consecutive serial sections. For four of the embryos, the presence of a single arterial common trunk, which was a direct continuation of the outflow tract and from which both the coronary arteries and the pulmonary arteries originated, was confirmed (Fig. 6E to G). In one other embryo, a single arterial common trunk was observed with coronary arteries but without pulmonary arteries. As a consequence, the tissue in the central areas of the right and left lungs showed obvious signs of hemorrhagic infarction and necrosis (Fig. 6H). In the last remaining embryo, we observed a condition known as double outlet right ventricle. Two arterial vessels originated from the right ventricle and could be identified as the aorta and pulmonary trunk by the respective presence of coronary and pulmonary arteries. The pulmonary trunk showed a stenosis with a marked reduction in its diameter compared to that of the adjacent aorta (Fig. 6I). An arterial duct was not observed in this embryo. It is known that the formation of the definitive ventriculo-arterial junction from the long, slowly conducting myocardial structure of the preseptation heart requires extensive remodeling of the outflow tract tissues. This appears to be severely disturbed in the absence of *Sox11*.

Cranial skeletal malformations. Approximately 70% of all *Sox11*-deficient embryos exhibited extensive clefting of the upper jaw and lips (Fig. 7A to C). This cleft was either unilateral or bilateral and resulted from a failure of the maxillary processes to fuse with the intermaxillary segment of the merged nasal prominences (Fig. 7I and J). Additionally, all mice with a cleft jaw and lip exhibited a cleft palate (Fig. 7D to F). The primary palate and secondary palate remained separate. In *Sox11*-deficient mice with a cleft lip and jaw, the palatine shelves of the maxillary bones failed to fuse along the entire length of the midline (Fig. 7G and H). Skeletal preparations of embryos at 18.5 dpc revealed that the maxillary bones and palatine shelves were strongly underdeveloped (Fig. 7K and L), whereas the mandible was essentially normal in size and shape. Additional defects were visible in the pterygoid process of the basisphenoid bone. In *Sox11*-deficient mice without visible lip and jaw clefting, the palatine shelves often failed to fuse

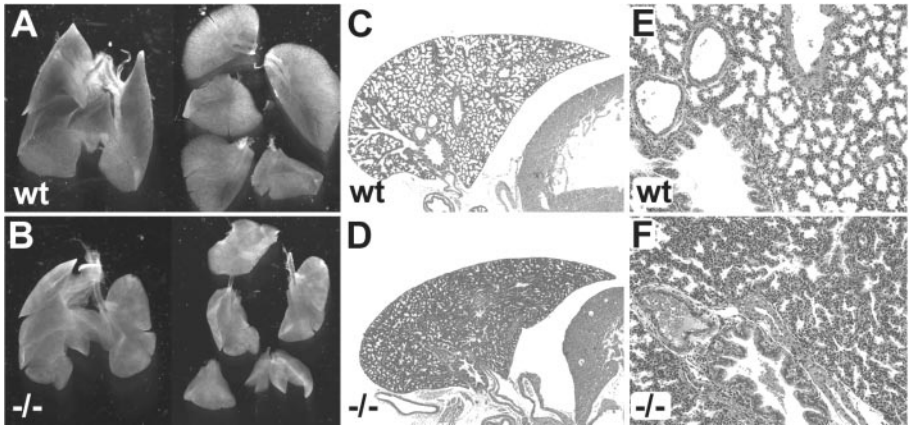

FIG. 4. Lung hypoplasia in *Sox11*-deficient mice. (A and B) Appearance of the lung and the five separate lung lobes at 18.5 dpc. In counterclockwise orientation starting at the top, the lobes are as follows: cranial right lobe, middle right lobe, caudal right lobe, accessory right lobe, and left lobe. (C to F) Hematoxylin-eosin staining of paraffin-embedded sections of the left lobe at low (C and D) and high (E and F) magnifications. (A, C, and E) Wild-type embryo; (B, D, and F) severely affected *Sox11*-deficient littermate. Note that neither embryo had breathed and that the lungs had not been inflated with air.

with the primary palate and with each other in the anterior part (Fig. 7E).

Additionally, ossification of several cranial bones was strongly reduced (Fig. 7I to N). Bones formed by endochondral ossification were affected as much as bones formed by intramembranous ossification. Bone sizes and bone densities were both decreased, and the matrix deposition rate was lowered, as shown paradigmatically for the interparietal bone (Fig. 7M and N). Sutures and fontanelles were enlarged correspondingly. At 18.5 dpc, separate ossification centers could still be recognized in the parietal bones (data not shown); ossification in the cartilage primordium of the supraoccipital bone was rudimentary in the Sox11-deficient embryos.

Noncranial skeletal malformations. Bone defects were also observed in various parts of the skeleton. All 10 skeletal preparations of *Sox11*-deficient embryos at 18.5 dpc exhibited severe abnormalities of the sternum and ribs (Fig. 8A to C). The sizes of all ossification centers in the sternebrae were reduced relative to the wild type. Usually, each sternebra possesses two cartilaginous precursor elements which fuse and form an individual sternebral cartilaginous unit, within which the sternebral ossification centers develop. In *Sox11*-deficient mice, the forth intercostal ossification center was rudimentary or completely absent at 18.5 dpc (Fig. 8B and C). In the first, second, and particularly the third sternebrae, two separate ossification centers of different sizes were often observed at either side of the midline, indicating that fusion of the cartilaginous precursor elements had not occurred (Fig. 8B and C). Often, the ossification centers were positioned asymmetrically, in extreme cases being completely out-of-step with their respective partners (Fig. 8A to C, insets). Contrary to the wild type, the two bilateral ossification centers of the xiphoid process had never fused. Sometimes they were different sizes (Fig. 8C) or were completely missing (Fig. 8B).

The attachment of the ribs to the sternum followed an irregular pattern, closely corresponding to the asymmetrical distribution of ossification centers along the sternum. Irregular insertion into the sternum notwithstanding, the rostral seven ribs were always attached to the sternum (Fig. 8A to C). Of the

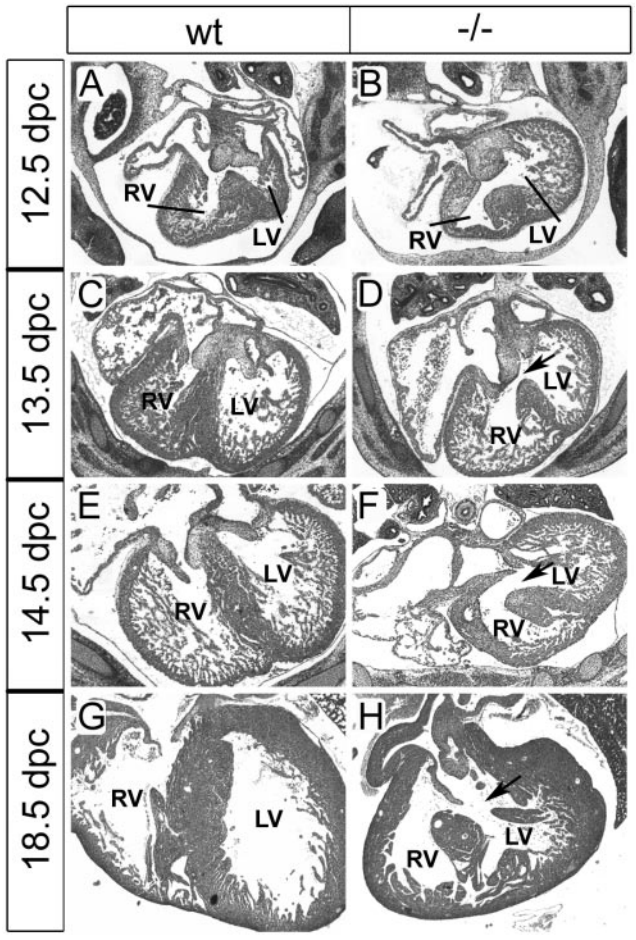

FIG. 5. Ventricular septation defects in *Sox11*-deficient mice. Hematoxylin-eosin-stained paraffin-embedded sections (horizontal plane) of the heart at atrioventricular valve levels in wild-type embryos (wt) and age-matched *Sox11*-deficient littermates (−/−) at 12.5, 13.5, 14.5, and 18.5 dpc. From 13.5 dpc onwards, the ventricular septum should completely separate the left ventricle (LV) from the right ventricle (RV). Arrows mark the ventricular septation defect.

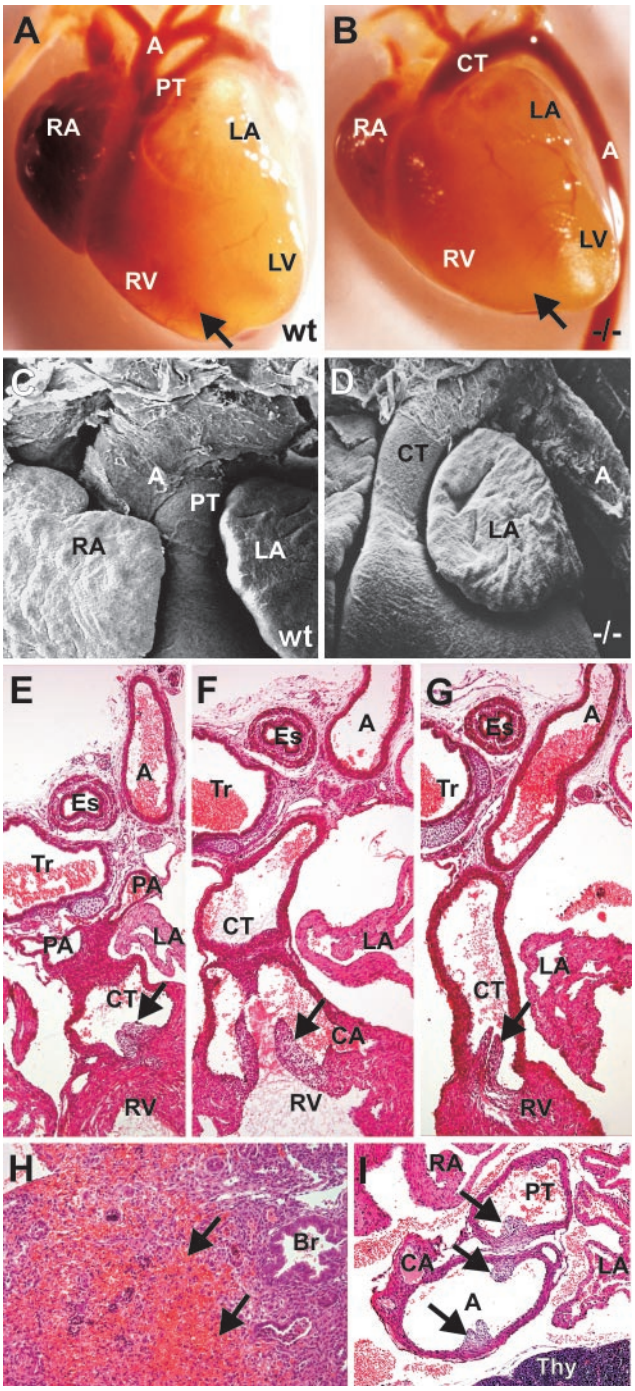

FIG. 6. Developmental defects of cardiac outflow tract in *Sox11*-deficient mice. (A to D) Outer appearance of the heart in wild-type (wt) embryos (A and C) and *Sox11*-deficient (−/−) littermates (B and D) at 18.5 dpc, as recorded by light (A and B) and scanning electron (C and D) microscopy. In wild-type embryos, the pulmonary trunk (PT) and aorta (A) were clearly separated and originated from their typical positions. In *Sox11*-deficient embryos, a single arterial common trunk (CT) that originated from the right ventricle (RV) and was continuous with the descending aorta (A), which was situated on the left side, was observed. Arrows in panels A and B mark the interventricular sulcus. RA, right atrium; LA, left atrium; LV, left ventricle. (E and F) Histology of consecutive serial sections (horizontal plane) of the cardiac outflow tract in *Sox11*-deficient embryos at 18.5 dpc. A common arterial trunk (CT) continues from the right ventricle (RV). Pulmonary arteries (PA) and coronary arteries (CA) originate from the common trunk (E and F), which is continuous with the descending aorta (G). A, aorta; Es, esophagus; Tr, trachea; LA, left atrium. Arrows mark the positions of the semilunar valves. (H) Hemorrhagic infarction and necrosis in the lung of a *Sox11*-deficient embryo (18.5 dpc), with a complete absence of pulmonary arteries. Br, bronchiole. (I) Stenosis of the pulmonary trunk (PT) in a *Sox11*-deficient embryo at 18.5 dpc. A, aorta; CA, coronary artery; RA, right atrium; Thy, thymus. Arrows mark the positions of the semilunar valves.

remaining six caudal ribs, all appeared to be normal, with the exception of the most caudal one. The 13th pair of ribs often had a reduced size. In one embryo, this pair of ribs was completely missing (Fig. 8D, left panel). Instead, rudiments of a 14th rib were found on the first lumbar vertebra, thus partly transforming the first lumbar into an additional thoracic vertebra. A 14th rib was also found in a second embryo in which all 13 regular pairs of ribs were present, arguing that the presence of a supernumerary rib rudiment is not strictly coupled to the absence of the 13th rib (Fig. 8D, right panel). Furthermore, all of the animals exhibited an abnormal curvature of the ribs, resulting in the formation of a barrel chest. Abnormal ventral curvature was also frequently observed for the clavicles of *Sox11*-deficient embryos (Fig. 8K).

Ossification defects additionally occurred in several vertebrae, particularly in the lumbar region, but also in the thoracic and sacral regions. Instead of a single ossification center in the vertebral body, we often observed two separate ossification centers or two ossification centers in various stages of fusion on both sides of the midline (Fig. 8E and F). A comparison of alcian blue and alizarin red staining revealed that already the cartilage, not just the bone, was separated in the affected vertebrae. Malformations in caudal vertebrae, including the fusion of adjacent vertebrae (Fig. 8G), are responsible for the curled tail observed in 15% of *Sox11*-deficient mice obtained at late stages of embryogenesis (Fig. 8H).

A general delay in endochondral ossification was particularly evident from analyses of hindlimbs at 18.5 dpc (Fig. 8I and J). Relative to those of age-matched wild-type embryos, the condensing bones of all phalanges were either reduced in size or even absent at 18.5 dpc in *Sox11*-deficient embryos. Similarly, ossification of the calcaneus and the talus was delayed.

Abdominal defects. Some Sox11-deficient embryos also exhibited a persistent herniation of the gut (Fig. 9A and B). This omphalocele occurs transiently as a normal physiological process at midgestation. Starting at 12.0 dpc, the rapidly enlarging visceral organs herniate into the root of the umbilical cord to escape the limiting space of the peritoneal cavity. After expansion of the peritoneal cavity, retraction of the visceral organs from the umbilical cord should be completed by 16.5 dpc. As expected, wild-type embryos showed complete resolution of the physiological omphalocele by embryonic day 18.5 (Fig. 9A). In contrast, 35% of all Sox11-deficient embryos analyzed displayed an omphalocele at this embryonic age. The sac contained either the intestine alone or the liver in addition to the intestine (Fig. 9B and data not shown).

An inspection of the abdominal organs in Sox11-deficient embryos also revealed a fully penetrant asplenia during late embryogenesis (Fig. 9C to F). The spleen normally forms from condensations of coelomic epithelium and the underlying mes-

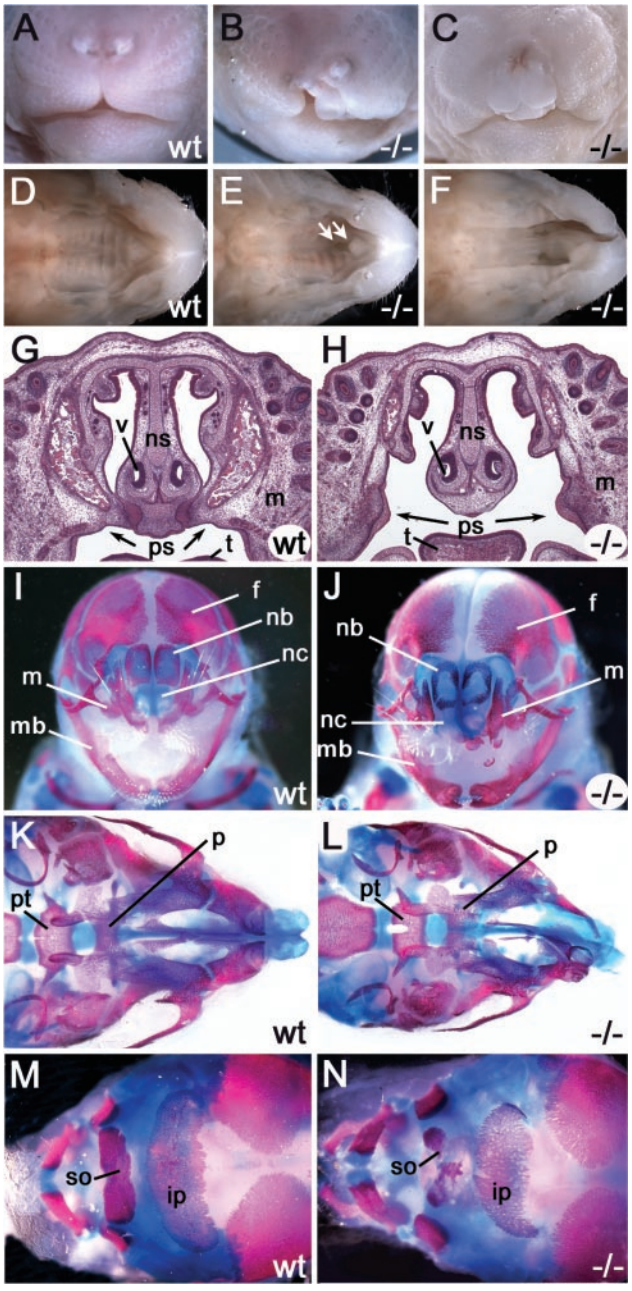

FIG. 7. Cleft palate and cranial malformations in *Sox11*-deficient embryos. (A to F) Outer appearance of snout (A to C [frontal view]) and palate (D to F [ventral view after removal of mandibles]) in wild-type (A and D) and *Sox11*-deficient (B, C, E, and F) embryos at 18.5 dpc. The cleft lip in *Sox11*-deficient embryos can be one-sided (B) or two-sided (C) and is associated with a cleft palate (F). Arrows in panel E mark the mild palatal cleft observed in a *Sox11*-deficient embryo without an obvious cleft lip. (G and H) Histology of coronal sections of wild-type (wt) and *Sox11*-deficient (−/−) heads at 18.5 dpc. (I to N) Alizarin red and alcian blue staining of cranial bones and cartilage in wild-type (wt) embryos (I, K, and M) and *Sox11*-deficient (−/−) littermates (J, L, and N) at 18.5 dpc. (I and J) Frontal view of skull; (K and L) ventral view of skull; (M and N) dorsal view of skull. Abbreviations: f, frontal bone; ip, interparietal bone; m, maxilla; mb, mandible; nb, nasal bone; nc, nasal capsule; ns, nasal septum; p, palatine bone; ps, palatal shelves; pt, pterygoid bone; so, supraoccipital bone; t, tongue; v, vomeronasal organ.

enchyme of the dorsal mesogastrium. In wild-type embryos, the splenic primordium is morphologically first identifiable as a ridge of cells immediately dorsal to the stomach at 13.5 dpc. In contrast, this splenic primordium was not anatomically detectable in age-matched *Sox11*-deficient embryos at 13.5 dpc (data not shown), arguing that spleen organogenesis is disrupted at an early point, before lymphocytes are recruited and splenogenesis progresses through cross-interactive signaling between lymphocytes and splenic mesenchymal cells. Additionally, the stomach and pancreas were found to be hypomorphic (Fig. 9C to F). Within the stomach, caudal parts such as the pylorus and corpus appeared most strongly affected. The pyloric constriction was malformed.

DISCUSSION

During mouse embryogenesis, the high-mobility-group transcription factor Sox11 exhibits a wide and highly dynamic expression pattern (14, 17). Most conspicuous is the near ubiquitous occurrence of Sox11 during early embryogenesis. Therefore, *Sox11*-deficient mice might have been predicted to exhibit early embryonic lethality. However, they reached birth but died shortly thereafter from congenital cyanosis. At this time, *Sox11*-deficient mice exhibited severe defects in several organ systems which all express *Sox11* at times of extensive remodeling (14, 17). Table 1 summarizes the various phenotypic defects and the frequencies at which they occur in *Sox11*-deficient mice. We also noted a 23% weight reduction at the time of birth. This overall growth retardation may be linked to the early ubiquitous expression of *Sox11* or secondary to the various organ malformations and ensuing suboptimal growth conditions.

Of the many developmental defects observed in Sox11-deficient mice, those concerning the heart most likely lead to early perinatal death because of their severity and complete penetrance. All mice analyzed exhibited a ventricular septation defect that was closely associated with outflow tract malformations that ranged from common arterial trunk to double outlet right ventricle. Similar heart phenotypes have been observed in many different knockout mice and have been found to be incompatible with postnatal life (1, 5, 13, 23, 34).

A heart phenotype was not necessarily expected, as the heart is the only main organ system from which Sox11 is conspicuously absent in the early postgastrulation embryo (14, 17). Additionally, mice deficient for the highly related *Sox4* already exhibit severe defects in the outflow tract region of the heart (25, 34). The fact that similar heart defects were observed in both *Sox4*- and *Sox11*-deficient mouse models is compatible with different explanations. It is possible that Sox4 and Sox11 are required within the same cells. Taking the high degree of sequence conservation and the similar biochemical properties into account (17), both proteins might contribute to a common function in an additive and partially redundant manner. It can also be envisaged that one Sox protein regulates the expression of the other. Given the fact that *Sox4*-deficient mice exhibit a more severe phenotype, Sox4 may regulate *Sox11* expression. There is precedence for such an epistatic relationship between structurally related Sox proteins, as Sox9 has been shown to activate the expression of the related group E Sox protein Sox8 in Sertoli cells of the male gonad (6).

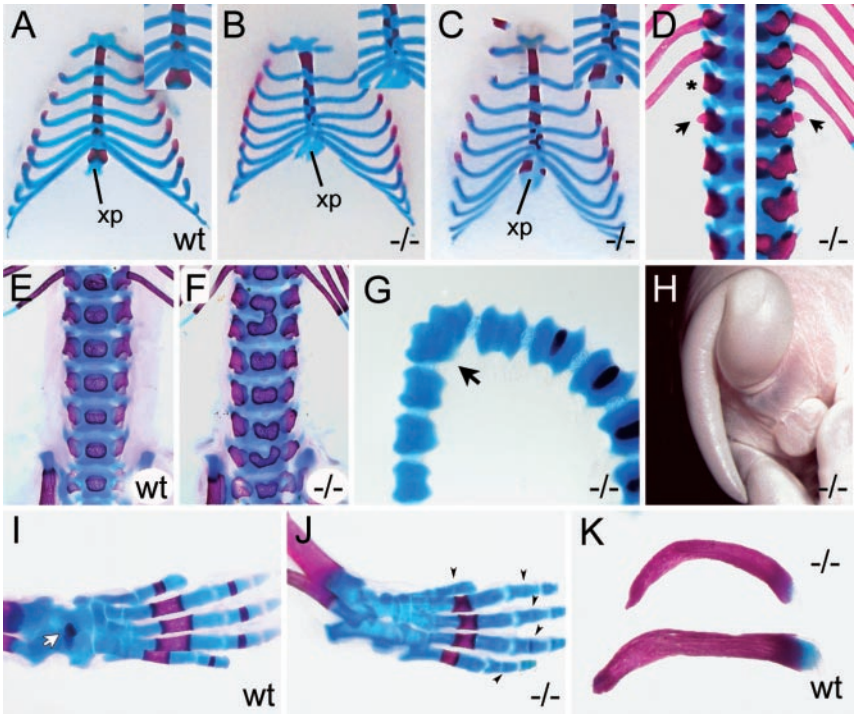

FIG. 8. Skeletal malformations in *Sox11*-deficient embryos. (A to C) Alizarin red (bone) and alcian blue (cartilage) staining of rib cages (ventral view) of wild-type (wt) embryo (A) and *Sox11*-deficient (−/−) littermates (B and C) at 18.5 dpc. Insets show magnifications of the caudal sternum. xp, xiphoid process of sternum. (D) Alizarin red (bone) and alcian blue (cartilage) staining of spinal column (dorsal view) of *Sox11*-deficient embryos at 18.5 dpc at thoracolumbar level. The asterisk marks the missing 13th rib. Arrows point to additional rib studs on the first lumbar vertebra. Two spinal columns are shown, with each being half-sided. (E and F) Lumbar spinal columns of wild-type (wt) and *Sox11*-deficient embryos at 18.5 dpc from the ventral aspect showing malformations of vertebral bodies. (G and H) Kinked tail of *Sox11*-deficient mouse at 18.5 dpc shown by alizarin red and alcian blue staining (G) and by outer appearance (H). The arrow in panel G points to the fused caudal vertebrae. (I and J) Hindlimbs of wild-type (wt) and *Sox11*-deficient (−/−) mice at 18.5 dpc showing reduced bone formation of talus (white arrow in panel I) and phalanges (black arrowheads in panel J). (K) Clavicles from *Sox11*-deficient (−/−) (top) and wild-type (wt) (bottom) siblings at 18.5 dpc showing abnormal ventral curvature of the *Sox11*-deficient clavicle.

Alternatively, expression of the two related Sox proteins may occur in different or only partially overlapping cell populations or during different developmental phases in the outflow tract region of the heart. Outflow tract defects of the kind observed in *Sox11*-deficient mice can be caused by mutations in genes expressed in endocardial cells or in cardiac neural crest cells, which both contribute to the outflow tract tissue and participate in the extensive remodeling that leads to the formation of the definitive arterio-ventricular junction (8). Favoring the existence of separate expression domains for Sox4 and Sox11 in the heart is the fact that Sox4 is believed to be expressed primarily in endocardially derived cells (34), whereas Sox11 is detectable at early phases in the cardiac neural crest (14). However, Sox11 also occurs later in endocardial cells.

Interestingly, Sox11 is widely expressed in cells of the neural crest and in many of its derivatives. In addition to the cardiac neural crest, Sox11 is present in the cranial, vagal, and trunk neural crests. Its strong expression in the cranial crest correlates with the occurrence of several craniofacial defects, including delayed intramembranous ossification of the cranial bones, clefting of the lip, jaw, and palate, and eyelid closure defects. However, Sox11 expression in the craniofacial area is not restricted to neural crest-derived cells. Thus, it is difficult to decide whether developmental defects in the cranial neural crest are the primary cause for the observed malformations. Similarly, it is difficult to distinguish between cell-autonomous and non-cell-autonomous defects in the cranial neural crest. A mixture of both has recently been shown for the transcription factor AP-2α (4). Although the loss of AP-2α was originally believed to primarily affect the neural crest (26, 35), neural crest-specific inactivation only led to a subset of the phenotypes observed in the constitutive *AP-2*α-deficient mouse, thus arguing for both cell-autonomous and non-cell-autonomous functions.

It should be mentioned that the related Sox4 protein is also expressed in pharyngeal arches and the craniofacial mesenchyme (14, 17). However, due to the early embryonic lethality of *Sox4*-deficient mice, it is unknown at present whether Sox4 is similarly needed for craniofacial development.

Developmental defects in *Sox11*-deficient mice are not confined to tissues with a significant neural crest contribution. An omphalocele, for instance, affects the junction between the surface ectoderm and the amnion and is caused by defective development of the anterior abdominal wall and failed umbilical ring closure (16). Interestingly, an omphalocele has also been observed in mice deficient for *AP-2*α (35). Thus, the phenotypic overlap of *Sox11*- and *AP2*α-deficient mice is not restricted to defects associated with neural crest development, suggesting that these two transcription factors affect a general developmental pathway in a similar manner.

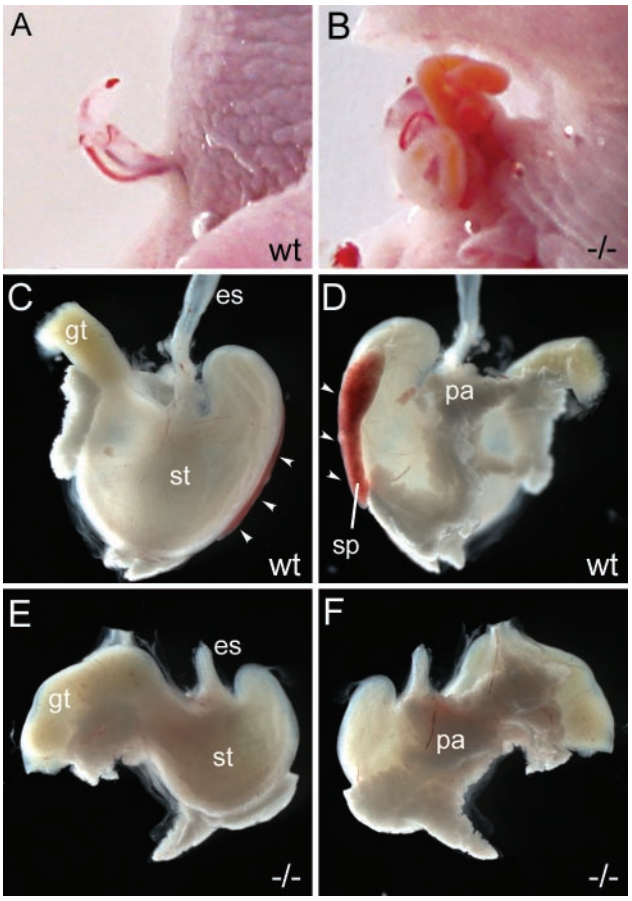

FIG. 9. Abdominal wall closure defects, asplenia, and stomach hypoplasia in Sox11-deficient embryos. (A and B) Abdominal body wall malformations in *Sox11*-deficient mice (B) compared to their control littermates (A) at 18.5 dpc. (C to F) Appearance of stomach (st) with spleen (sp; white arrowheads) and pancreas (pa) of wild-type (C and D) and *Sox11*-deficient (E and F) mice at 18.5 dpc from ventral (C and E) and dorsal (D and F) aspects. es, esophagus; gt, gut.

Malformations of the axial skeleton affect mesodermal cells. The delayed endochondral ossification observed in Sox11-deficient mice, as well as the irregularities of the ribs, sternum, and vertebrae, has also been reported in various combinations for several other mouse mutants (10, 13, 23, 32). The spleen is also derived from mesoderm, as it develops from a condensation of coelomic epithelium and the underlying mesenchyme.

TABLE 1. Summary of phenotypes and their frequencies of occurrence in *Sox11*-deficient mice (16.5 to 18.5 dpc)

Phenotype	% of affected $Sox11^{-/-}$ mice	No. of analyzed $Sox11^{-/-}$ mice
Congenital cyanosis	100	62
Ventricular septation defect	100	9
Cardiac outflow tract malformations	100	15
Cleft lip and/or jaw	69	62
Skeletal malformations	100	10
Asplenia	100	27
Eyelid closure	97	62
Omphalocele	35	62
Curled tail	15	62

Asplenia in *Sox11*-deficient mice is therefore likely caused by defects in either of these two components or in their interaction. The molecular mechanism leading to asplenia is not yet clear. However, the defect occurs early, as a morphologically visible spleen anlage does not form. This is similarly observed in mice deficient for *capsulin*/*epicardin*/*Pod-1*, *Nkx3.2*/*Bapx1*, or *Hox11* (9, 19, 29). In *Sox11*-deficient mice, the defect is not restricted to the spleen, as other derivatives of the splanchnic mesoderm, such as the pancreas, also appear to be affected, although to a lesser extent.

The common denominator of all affected tissues is that they have to undergo extensive remodeling during development, which suggests that there is a link between Sox11 and tissue remodeling. In light of this assumption, strong *Sox11* expression in the neural crest might be a consequence of the fact that these cells are often involved in remodeling. These processes involve complicated and poorly understood reciprocal intercellular signaling processes, often in the form of epithelial-mesenchymal inductions. During these processes, several signal transduction pathways are active, including Wnt, transforming growth factor beta (TGF-β), bone morphogenetic protein, fibroblast growth factor, and Hedgehog signaling. If Sox11 participates in tissue remodeling, it should be part of these signal transduction pathways. As a consequence, phenotypes between *Sox11*-deficient mice and mice with mutations in components of these pathways should overlap, and this is indeed the case (1, 10, 13, 20). The highest phenotypic concordance with Sox11-deficient mice is observed for mice lacking *TGFβ2* (23). The inactivation of *TGFβ2* leads to highly similar heart and lung defects. Additionally, both mouse mutants exhibit severe craniofacial malformations. These include palatal clefting as well as abnormal intramembranous or endochondral ossification of several cranial bones. However, there are also minor differences, with the mandibles only being affected in *TGFβ2*-deficient mice and cleft lip only being observed in *Sox11*-deficient mice. There is also a significant, though not complete, overlap in other skeletal malformations. In particular, sternum malformations, rib defects, and the abnormal curvature of the clavicles in the two mouse mutants are strongly reminiscent of each other. Omphalocele is observed in *Sox11*-deficient mice as well as in *TGFβ2*-deficient mice with an additional loss of *TGFβ3* (12). If we take the strong phenotypic overlap into account, Sox11 may be a component of the TGF-β2 signaling pathway.

Lastly, it should be mentioned that many of the phenotypes observed in Sox11-deficient mice occur frequently in humans. Heart defects, cleft palate, cleft lip, and omphalocele all range among the most frequent congenital birth defects. Congenital heart defects, for instance, occur in 1 of every 150 newborns, with ventricular septation defects diagnosed in 1 in 800 newborns and outflow tract malformations such as persistent truncus arteriosus exhibiting frequencies of 1 in 10,000 (2). Omphalocele, on the other hand, affects approximately 1 in 3,500 children (16). Frequencies of cleft lip range from 1 in 300 to 1 in 2,500 (with or without cleft palate), whereas isolated cleft palate is found in approximately 1 in 1,500 newborns (33). The occurrence of all of these defects can be sporadic or familial and syndromic or nonsyndromic. In some of the syndromic cases, craniofacial abnormalities, heart defects, and omphalocele even occur together or in various combinations

with other phenotypes, including some that are found in *Sox11*-deficient mice, such as skeletal malformations and asplenia. Although no syndromic form of cleft palate, cleft lip, or congenital heart defect has yet been mapped to the chromosomal location of the human *SOX11* gene on 2p25 (15), SOX11 is clearly a good candidate to be affected in such syndromes with so far unknown genetic etiologies.

ACKNOWLEDGMENTS

We thank Gertrud Link and Elke Kretzschmar for expert technical assistance.

This work was funded by a Fonds der Chemischen Industrie grant to M.W.

REFERENCES

1. **Abu-Issa, R., G. Smyth, I. Smoak, K.-I. Yamamura, and E. N. Meyera.** 2002. Fgf8 is required for pharyngeal arch and cardiovascular development in the mouse. Development **129:**4613–4625.
2. **Bernstein, E.** 2004. The cardiovascular system, p. 413–437. *In* R. E. Behrman, R. M. Kliegman, and A. M. Arvin (ed.), Nelson textbook of pediatrics, 17th ed. Saunders, Philadelphia, Pa.
3. **Bowles, J., G. Schepers, and P. Koopman.** 2000. Phylogeny of the SOX family of developmental transcription factors based on sequence and structural indicators. Dev. Biol. **227:**239–255.
4. **Brewer, S., W. Feng, J. Huang, S. Sullivan, and T. Williams.** 2004. Wnt1-Cre-mediated deletion of AP-2alpha causes multiple neural crest-related defects. Dev. Biol. **267:**132–152.
5. **Brewer, S., X. Jiang, S. Donaldson, T. Williams, and H. M. Sucov.** 2002. Requirement for AP-2α in cardiac outflow tract morphogenesis. Mech. Dev. **110:**139–149.
6. **Chaboissier, M.-C., A. Kobayashi, V. I. P. Vidal, S. Lützkendorf, H. J. G. van de Kant, M. Wegner, D. G. de Rooij, R. R. Behringer, and A. Schedl.** 2004. Functional analysis of Sox8 and Sox9 during sex determination in the mouse. Development **131:**1891–1901.
7. **Cheung, M., M. Abu-Elmagd, H. Clevers, and P. J. Scotting.** 2000. Roles of Sox4 in central nervous system development. Mol. Brain Res. **79:**180–191.
8. **Conway, S. J., A. Kruzynska-Frejtag, P. L. Kneer, M. Machniki, and S. V. Koushik.** 2003. What cardiovascular defect does my prenatal mouse mutant have, and why? Genesis **35:**1–21.
9. **Dear, T. N., W. H. Colledge, M. B. L. Carlton, I. Lavenir, T. Larson, A. J. H. Smith, A. J. Warren, M. J. Evans, M. V. Sofroniew, and T. H. Rabbitts.** 1995. The Hox11 gene is essential for cell survival during spleen development. Development **121:**2909–2915.
10. **Delot, E. C., M. E. Bahamonde, M. Zhao, and K. M. Lyons.** 2003. BMP signaling is required for septation of the outflow tract of the mammalian heart. Development **130:**209–220.
11. **de Martino, S., Y. L. Yan, T. Jowett, J. H. Postlethwait, Z. M. Varga, A. Ashworth, and C. A. Austin.** 2000. Expression of sox11 gene duplicates in zebrafish suggests the reciprocal loss of ancestral gene expression patterns in development. Dev. Dyn. **217:**279–292.
12. **Dünker, N., and K. Krieglstein.** 2002. TGFβ2$^{-/-}$ TGFβ3$^{-/-}$ double knockout mice display severe midline fusion defects and early embryonic lethality. Anat. Embryol. **206:**73–83.
13. **Hamblet, N. S., N. Lijam, P. Ruiz-Lozano, J. Wang, Y. Yang, Z. Luo, L. Mei, K. R. Chien, D. J. Sussman, and A. Wynshaw-Boris.** 2002. Dishevelled 2 is essential for cardiac outflow tract development, somite segmentation and neural tube closure. Development **129:**5827–5838.
14. **Hargrave, M., E. Wright, J. Kun, J. Emery, L. Cooper, and P. Koopman.** 1997. Expression of the Sox11 gene in mouse embryos suggests roles in neuronal maturation and epithelio-mesenchymal induction. Dev. Dyn. **210:** 79–86.
15. **Jay, P., C. Goze, C. Marsollier, S. Taviaux, J.-P. Hardelin, P. Koopman, and P. Berta.** 1995. The human Sox11 gene: cloning, chromosomal assignment and tissue expression. Genomics **29:**541–545.
16. **Kilby, M. D., A. Lander, and M. Usher-Somers.** 1998. Exomphalos (omphalocele). Prenat. Diagn. **18:**1283–1288.
17. **Kuhlbrodt, K., B. Herbarth, E. Sock, J. Enderich, I. Hermans-Borgmeyer, and M. Wegner.** 1998. Cooperative function of POU proteins and Sox proteins in glial cells. J. Biol. Chem. **273:**16050–16057.
18. **Lioubinski, O., M. Müller, M. Wegner, and M. Sander.** 2003. Expression of *Sox* transcription factors in the developing mouse pancreas. Dev. Dyn. **227:** 402–408.
19. **Lu, J., P. Chang, J. A. Richardson, L. Gan, H. Weiler, and E. N. Olson.** 2000. The basic helix-loop-helix transcription factor capsulin controls spleen organogenesis. Proc. Natl. Acad. Sci. USA **97:**9525–9530.
20. **Matzuk, M. M., T. R. Kumar, and A. Bradley.** 1995. Different phenotypes for mice deficient in either activins or activin receptor type II. Nature **374:**356–360.
21. **Miyata, S., K. Miyashita, and Y. Hosoyama.** 1996. Sry-related genes in Xenopus oocytes. Biochim. Biophys. Acta **1308:**23–27.
22. **Rimini, R., M. Beltrame, F. Argenton, D. Szymczak, F. Cotelli, and M. E. Bianchi.** 1999. Expression patterns of zebrafish sox11A, sox11B and sox21. Mech. Dev. **89:**167–171.
23. **Sanford, L. P., I. Ormsby, A. C. Gittenberger-de Groot, H. Sariola, R. Friedman, G. P. Boivin, E. L. Cardell, and T. Doetschman.** 1997. TGFβ2 knockout mice have multiple developmental defects that are non-overlapping with other TGFβ knockout phenotypes. Development **124:**2659–2670.
24. **Schilham, M. W., P. Moerer, A. Cumano, and H. C. Clevers.** 1997. Sox-4 facilitates thymocyte differentiation. Eur. J. Immunol. **27:**1292–1295.
25. **Schilham, M. W., M. A. Oosterwegel, P. Moerer, J. Ya, P. A. J. Deboer, M. Vandewetering, S. Verbeek, W. H. Lamers, A. M. Kruisbeek, A. Cumano, and H. Clevers.** 1996. Defects in cardiac outflow tract formation and pro-B-lymphocyte expansion in mice lacking Sox-4. Nature **380:**711–714.
26. **Schorle, H., P. Meier, M. Buchert, R. Jaenisch, and P. J. Mitchell.** 1996. Transcription factor AP-2 essential for cranial closure and craniofacial development. Nature **381:**235–238.
27. **Sock, E., K. Schmidt, I. Hermanns-Borgmeyer, M. R. Bösl, and M. Wegner.** 2001. Idiopathic weight reduction in mice deficient in the high-mobility-group transcription factor Sox8. Mol. Cell. Biol. **21:**6951–6959.
28. **Stolt, C. C., S. Rehberg, M. Ader, P. Lommes, D. Riethmacher, M. Schachner, U. Bartsch, and M. Wegner.** 2002. Terminal differentiation of myelin-forming oligodendrocytes depends on the transcription factor Sox10. Genes Dev. **16:**165–170.
29. **Tribioli, C., and T. Lufkin.** 1999. The murine Bapx1 homeobox gene plays a critical role in embryonic development of the axial skeleton and spleen. Development **126:**5699–5711.
30. **Uwanogho, D., M. Rex, E. J. Cartwright, G. Pearl, C. Healy, P. J. Scotting, and P. T. Sharpe.** 1995. Embryonic expression of the chicken Sox2, Sox3 and Sox11 genes suggests an interactive role in neuronal development. Mech. Dev. **49:**23–36.
31. **Wegner, M.** 1999. From head to toes: the multiple facets of Sox proteins. Nucleic Acids Res. **27:**1409–1420.
32. **Wurst, W., A. B. Auerbach, and A. L. Joyner.** 1994. Multiple developmental defects in Engrailed-1 mutant mice: an early mid-hindbrain deletion and patterning defects in forelimbs and sternum. Development **120:**2065–2075.
33. **Wyszynski, D. F., T. H. Beaty, and N. E. Maestri.** 1996. Genetics of nonsyndromic oral clefts revisited. Cleft Palate Craniofac. J. **33:**406–417.
34. **Ya, J., M. W. Schilham, P. A. J. de Boer, A. F. M. Moorman, H. Clevers, and W. H. Lamers.** 1998. Sox4-deficiency syndrome in mice is an animal model for common trunk. Circ. Res. **83:**986–994.
35. **Zhang, J., S. Hagopian-Donaldson, G. Serbedzija, J. Elsemore, D. Plehn-Dujowich, A. P. McMahon, R. A. Flavell, and T. Williams.** 1996. Neural tube, skeletal and body wall defects in mice lacking transcription factor AP-2. Nature **381:**238–241.